Pliocene eclogite exhumation at plate tectonic rates in eastern Papua New Guinea

Suzanne L. Baldwin[1], Brian D. Monteleone[1], Laura E. Webb[1], Paul G. Fitzgerald[1], Marty Grove[2] & E. June Hill[3]

[1]*Syracuse University, Department of Earth Sciences, Syracuse, New York 13244, USA*
[2]*University of California at Los Angeles, Department of Earth and Space Sciences, Los Angeles, California 90095, USA*
[3]*Commonwealth Scientific and Industrial Research Organization, Petroleum Resources, 26 Dick Perry Avenue, Kensington, Western Australia 6151, Australia*

As lithospheric plates are subducted, rocks are metamorphosed under high-pressure and ultrahigh-pressure conditions to produce eclogites and eclogite facies metamorphic rocks. Because chemical equilibrium is rarely fully achieved, eclogites may preserve in their distinctive mineral assemblages and textures a record of the pressures, temperatures and deformation the rock was subjected to during subduction and subsequent exhumation. Radioactive parent–daughter isotopic variations within minerals reveal the timing of these events. Here we present *in situ* zircon U/Pb ion microprobe data that dates the timing of eclogite facies metamorphism in eastern Papua New Guinea at 4.3 ± 0.4 Myr ago, making this the youngest documented eclogite exposed at the Earth's surface. Eclogite exhumation from depths of ~75 km was extremely rapid and occurred at plate tectonic rates (cm yr^{-1}). The eclogite was exhumed within a portion of the obliquely convergent Australian–Pacific plate boundary zone, in an extending region located west of the Woodlark basin sea floor spreading centre. Such rapid exhumation (>1 cm yr^{-1}) of high-pressure and, we infer, ultrahigh-pressure rocks is facilitated by extension within transient plate boundary zones associated with rapid oblique plate convergence.

Oblique collision of major tectonic plates results in rapidly evolving plate boundaries that often exhibit a range of kinematic behaviour along strike as zones of deformation evolve from diffuse boundaries to discrete microplates[1]. The evolution of plate boundary zones involves the three-dimensional interplay between both continental and oceanic lithosphere, and mantle asthenosphere over geologic timescales. In Papua New Guinea (PNG), plate boundaries and microplates formed in response to the large-scale oblique collision of the Australian and Pacific plates[2,3] (Fig. 1). The region preserves a history of arc convergence, continent/arc collision, and ophiolite emplacement[4] followed by continental rifting and seafloor spreading[5]. In the western Woodlark basin of eastern PNG the transition from seafloor spreading to distributed extension occurs in the most rapidly extending active rift system on Earth[6,7]. West of the spreading centre, extensional movement on shear zones[8] led to the formation of metamorphic core complexes in the D'Entrecasteaux Islands[9,10] and resulted in the rapid exhumation of Pliocene plutonic and metamorphic rocks[11], including eclogites interpreted as having formed during prior subduction[12,13]. The plate boundary zone evolution can be examined in remnants of high-pressure rocks that have escaped overprinting by tectonic or thermal events during subsequent exhumation. We determine the age (4.3 ± 0.4 Myr), and exhumation at plate tectonic rates (tens of kilometres per million years), of the youngest known eclogite exhumed within the obliquely convergent Australian–Pacific (AUS–PAC) plate boundary zone of eastern PNG.

Eastern PNG plate boundary evolution

The present-day tectonic setting of PNG is the result of rapid (10–11 cm yr^{-1}) oblique AUS–PAC plate convergence[2,14–15] (Fig. 1). The AUS–PAC plate boundary zone is complex, has considerable along-strike variation, and has been a location for microplate formation and rotation, short-lived subduction and intraplate deformation[16,17]. Seismicity and GPS observations define at least three microplates in this convergent plate boundary zone: the Solomon Sea plate, and the North and South Bismark plates. On its northern boundary the Solomon Sea plate is subducting beneath the South Bismark plate at the New Britain trench. At its southern boundary the tectonic setting is less clear with seismic evidence having been used to argue both for[14,18] and against[19] southward subduction of the Solomon Sea plate beneath the Trobriand platform at the Trobriand trough. Interaction between the Australian plate and neighbouring microplates define a plate boundary zone presently characterized by arc-continent collision in the Huon peninsula region of PNG (AUS–South Bismark), seafloor spreading in the Woodlark basin (AUS–Woodlark), and possible subduction in the intervening region (Solomon Sea–Woodlark).

The Cenozoic evolution of this complex plate boundary zone involved northwards subduction of the Australian plate beneath the Pacific plate[4,17] that led to high-pressure metamorphism[12,13,20] of Jurassic–Cretaceous sediments and basalts, and southward obduction of oceanic crust and mantle of the Pacific plate to form the Papuan ultramafic belt[4,21] (Fig. 1). In eastern PNG the change from a dominantly convergent plate boundary to a dominantly divergent plate boundary resulted from counterclockwise rotation of the Solomon Sea plate[2] and ultimately led to seafloor spreading in the Woodlark basin. Since 6 Myr ago the Woodlark basin spreading centre has propagated westwards, separating the once contiguous Woodlark and Pocklington rises[6].

D'Entrecasteaux Island eclogites

The D'Entrecasteaux Island metamorphic core complexes[9,10] are located in a zone of extension west of the Woodlark basin spreading centre (Fig. 1). They consist of a lower plate of complexly deformed gneissic domes (up to 2.5 km above sea level), separated from an upper plate of largely undeformed mafic and ultramafic rocks[22] by shear zones and detachment faults[8]. The metamorphic basement is divided into two structural zones: a core zone and an outer shear zone[8,10]. The core zone consists of eclogites, migmatites, gneisses and mylonitic rocks. Although structural fabrics in the core zone are highly variable, an early deformation event (D_1) resulted in gneissic layering that predates peak metamorphism. A second generation of

deformation (D_2) postdates peak metamorphism and resulted in folding and boudinage of the gneissic layering and formation of retrograde tectonic fabrics associated with development of the outer sheared zone. The earliest retrograde fabrics formed during shearing under amphibolite facies conditions at pressures of 7–11 kbar and temperatures of 570–730 °C (ref. 13). Exhumation was facilitated by kilometre-scale mylonitic shear zones whose thermal histories are constrained by $^{40}Ar/^{39}Ar$ muscovite, biotite and feldspar, and apatite fission track ages[11,13].

Eclogite facies mineral assemblages preserve a high-pressure history and occur as variably retrogressed mafic lenses/layers in quartzofeldspathic gneisses, metamorphosed mafic dikes that cross-cut the D_1 gneissic fabric, and mafic xenoliths in Pliocene granodiorites. Major and trace element abundances are comparable with average MORB values[12]. Eclogites record metamorphic conditions that approached 24 kbar and 900 °C (refs 12,13). The eclogite analysed (sample 870921 from Fergusson Island; Fig. 1), preserves garnet ($Alm_{0.49}Py_{0.33}Gr_{0.17}Sp_{0.01}$; ~30%) + omphacite ($Jd_{0.57}$; ~40%) along with plagioclase + quartz (~5%) and retrograde amphibole (edenite–pargasite) + biotite (~15%) + chlorite (<5%). Accessory phases include rutile, titanite, apatite and zircon; many of these occur as inclusions within garnet. Omphacite also occurs as inclusions within garnet, as rims on garnet, and as relic grains within edenite–pargasite–plagioclase symplectite. Widespread rutile exsolution in garnet—common in isothermally decompressed high-pressure and ultrahigh-pressure (UHP) rocks[23]—occurs in this sample, although not in proximity to zircons analysed, or in the cores of garnet porphyroblasts. Within the matrix, rutile is rimmed by retrograde titanite and is intergrown with ilmenite.

Only omphacite and plagioclase inclusions within the core of a garnet porphyroblast were used for pressure–temperature (P–T) determinations. It is assumed that the omphacite and plagioclase inclusions were in local equilibrium with the encapsulating garnet and that element fractionation reflects ambient P–T conditions. Omphacite inclusions and adjacent garnet compositions indicate peak T conditions[24,25] of 870–930 °C. Plagioclase and omphacite inclusions within garnet indicate pressures of 20–24 kbar using the jadeite–albite–quartz barometer[26,27] (Fig. 2).

To determine the age of zircons in eclogite, *in situ* ion probe analyses were performed in thin section, allowing dating of zircons within a textural context with respect to the mineral paragenesis. The majority of the zircons analysed (for example, z2, z3, z4, z15, z26, z37) were relatively small (≤50 μm in longest dimension), elongate to rounded inclusions within garnet porphyroblasts (Fig. 3a). Zircons not enclosed in garnet include the largest zircon analysed (z33), a subhedral 300 μm × ~70 μm crystal within a retrograde amphibole (edenite–pargasite) and plagioclase ($Ab_{0.89–0.61}$) symplectite (Fig. 3a). Five analyses were obtained from different portions of this zircon (z33-1–5), with repeated drilling into some areas. Another zircon (z34) occurs within an amphibole rim on a garnet porphyroblast.

The age significance of U/Pb results (Fig. 3b) was determined by assuming that measured Pb was a simple mixture between a single concordant radiogenic endmember and common Pb. The zircons analysed gave a $^{238}U/^{206}Pb$ age of 4.33 ± 0.36 Myr (2σ; MSWD = 3.3) defined by the intersection with concordia of the best-fit line passing through the data. Because U-series disequilibrium would not shift the results by an amount in excess of the indicated errors[28], no corrections were necessary.

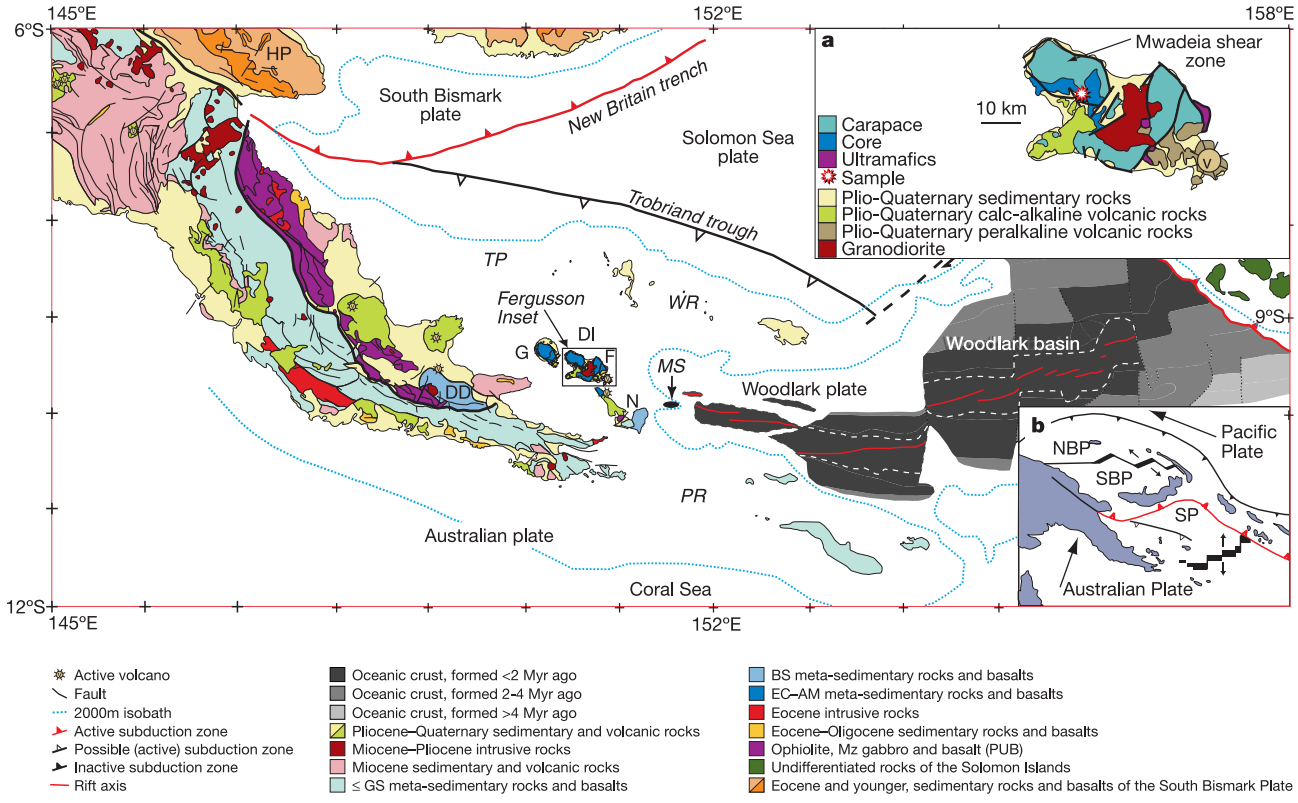

Figure 1 Eastern PNG tectonic and geologic maps[4,6,21]. DD, Dayman dome; DI, D'Entrecasteaux Islands; G, Goodenough Island; F, Fergusson Island; N, Normanby Island; MS, Moresby seamount; TP, Trobriand platform; WR, Woodlark rise; PR, Pocklington rise; HP, Huon peninsula. PUB, Papuan ultramafic belt; OC, oceanic crust; GS, greenschist; BS, blueschist; EC, eclogite; AM, amphibolite. **a**, Fergusson Island geology (see box on main figure labelled 'Fergusson Inset'; eclogite locality indicated[10]. Carapace, shear zones; core, gneiss, migmatite and eclogite. **b**, Australian–Pacific plate boundary zone microplates[2]. White dashed line indicates Bruhnes chron. NBP, North Bismark plate; SBP, South Bismark plate; SP, Solomon plate.

Interpreting U/Pb ages with respect to the eclogite's pressure–temperature–time–deformation (*P–T–t–D*) history requires establishing whether the zircon was inherited from the protolith, formed during subduction, or formed during exhumation. Lead diffusion in crystalline zircon is too slow to account for complete isotopic resetting of zircon inherited from a protolith[29]. Thus, given the relatively zirconium-poor bulk composition of the mafic protolith and the lack of identified zircon inheritance, zircon growth most probably occurred during metamorphic recrystallization. Neocrystallization of zircon during metamorphism at *P–T* conditions lower than upper amphibolite and granulite grade is rare[30]. Textural evidence indicates that most of the zircons were included within garnets (for example, z2, z3, z15, z26, z37). This textural relationship also argues against an interpretation of melt-controlled or fluid-controlled zircon growth. Other zircons occur in retrograde garnet rims (z34) and within symplectite.

To further constrain the *P–T* conditions under which the zircons formed, the trace element and rare earth element (REE) geochemistry of zircon and garnet were investigated by *in situ* ion microprobe analysis. Figure 3c shows chondrite-normalized[31] REE plots for zircon (z33) and adjacent garnet (grt33). Zircon exhibits a positive Ce anomaly relative to chondrite, an overall flat heavy REE pattern, and no significant negative Eu anomaly. Chondrite-normalized patterns for coexisting garnet do not reveal Ce or Eu anomalies. They have steeply positive profiles for Ce to Sm, and negatively sloping profiles for the heavy REE. Zircon/garnet distribution coefficients for the medium to heavy REE increase from 0.66 for Sm to 7.4 for Lu. The form of these REE patterns and the distribution coefficients are consistent with contemporaneous zircon/garnet growth and are remarkably similar to those determined for alpine eclogites[32,33].

The overall similarity to alpine eclogites and the lack of an Eu anomaly provide convincing evidence for zircon growth under eclogite facies conditions[33]. Retrograde formation of symplectic intergrowths after garnet + clinopyroxene involved significant plagioclase growth and would have induced a negative Eu anomaly in retrograde zircon. Hence we are confident in interpreting the $^{238}U/^{206}Pb$ age of 4.33 ± 0.36 Myr (2σ; MSWD = 3.3) as marking the time of zircon growth at eclogite facies conditions.

Exhumation rates

Since the Early Pliocene epoch, exhumation of this eclogite from a depth of approximately 75 km was facilitated by tectonic (that is, kilometre-scale mylonitic shear zones[8]) and erosional processes. We can use the boundary condition of the present-day surface of the Earth from which the sample was collected, the U/Pb zircon age and thermobarometric constraints to calculate average exhumation rates for this eclogite. This calculation does not rely on assumptions

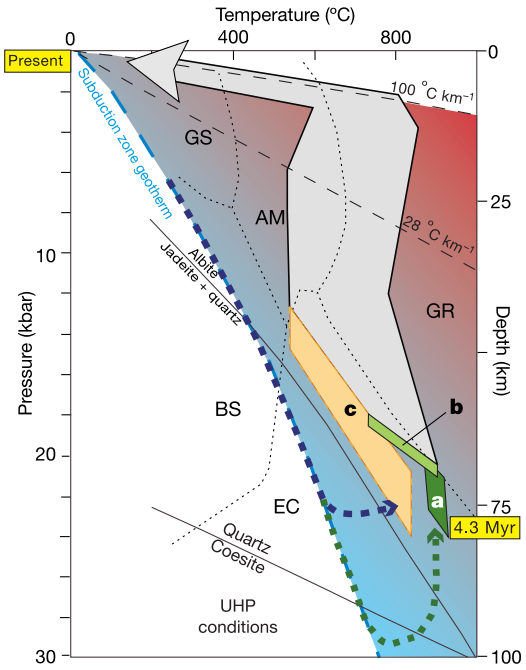

Figure 2 Pressure–temperature conditions for D'Entrecasteaux eclogites. **a**, This study; **b**, from ref. 10; **c**, from ref. 12. Exhumation path based on compilation of P–T data for eclogites, shear zone gneisses, and retrogressed core zone gneisses[13]. Two possible prograde paths for the eclogite are indicated as dashed lines with arrows. Metamorphic facies (abbreviations as in Fig. 1; GR, granulite), coesite = quartz, and jadeite + quartz = albite reaction curves indicated. Mineral compositions are given in the Supplementary Information. Subduction zone geotherm, and present-day range of thermal gradients from the Moresby seamount region[43], east of the D'Entrecasteaux Islands, are also shown.

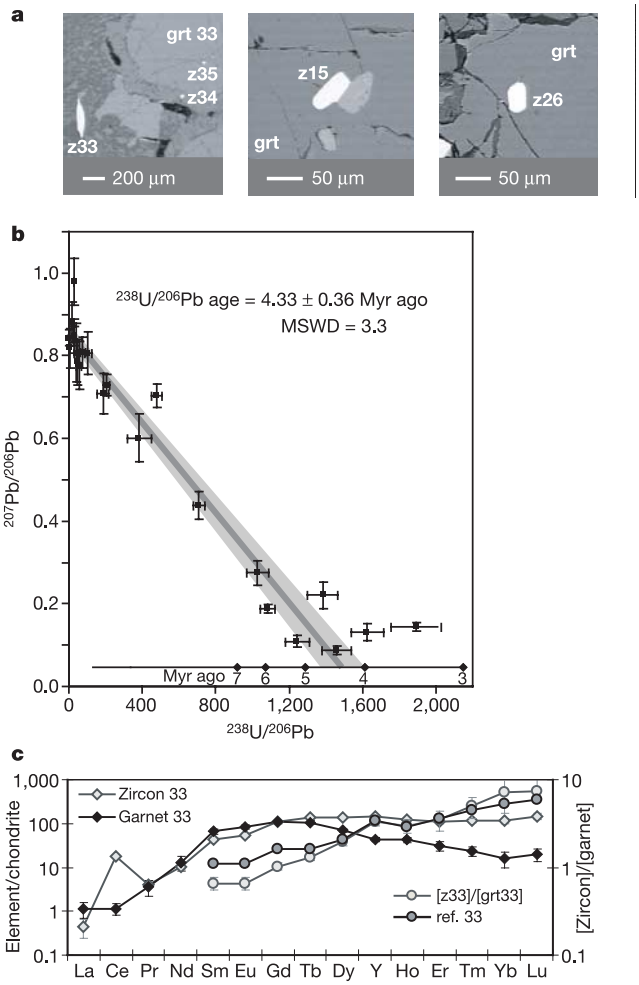

Figure 3 U/Pb, trace and REE results. **a**, Backscattered-electron images of selected zircons. Grt, garnet; z, zircon. **b**, Tera–Wasserburg plot with *in situ* U/Pb ion probe results. Individual analyses are plotted with 1σ errors. Regression (solid line) of U/Pb data, uncorrected for common Pb, indicates a $^{238}U/^{206}Pb$ age of 4.33 ± 0.36 Myr ago (2σ; MSWD = 3.3). Also shown is a 2σ error envelope on the regression. **c**, Trace element and REE data (average ± 1σ) for zircon (z33) and garnet (grt33), plotted relative to chondritic values[31]. Also shown are zircon/garnet distribution coefficients[33]. U–Th–Pb isotopic and REE data are provided in the Supplementary Information.

related to closure temperatures, or geothermal gradients. A minimum exhumation rate ($\sim$17 mm yr^{-1}) is calculated assuming vertical exhumation. A higher rate of 35–51 mm yr^{-1} is calculated given that the eclogite was at $\sim$75 km at 4.3 Myr ago, was exhumed from beneath the 20°–30° NNE dipping Mwadeia shear zone[8] and was collected from the Earth's surface (Figs 1 and 2). These average exhumation rates do not consider possible complicating effects such as trench migration and changes in the dip of the shear zone and/or subducting slab. Nor do these rates consider the extent to which mid-crustal flow contributed to changes in crustal thickness during the Australian–Solomon Sea/Woodlark plate boundary zone evolution, addition of mantle derived magmas to the base of the crust, variable exhumation mechanisms, or transient accelerations in exhumation rate. These average exhumation rates are, however, comparable to extension rates near the rift tip (25–40 mm yr^{-1}) (ref. 7), half-spreading rates determined both from magnetic reversals (20 and 26 mm yr^{-1}) (ref. 2) and GPS crustal motion surveys (12–40 mm yr^{-1}) (ref. 15) in the D'Entrecasteaux–Woodlark region.

At present we cannot constrain the *P–T–t* path followed by this sample before 4.3 Myr ago. If exhumed from UHP depths, 4.3 Myr ago marks the timing of retrograde high-pressure metamorphism (Fig. 2). Alternatively the sample may have reached peak pressure at 4.3 Myr ago and then was subsequently exhumed. Regardless of the details of the prograde path followed, the data presented provide compelling evidence for the existence of eclogite at depths of $\sim$75 km at 4.3 Myr ago. Movement on major crustal extensional shear zones facilitated exhumation of previously subducted, but largely buoyant crustal material, from beneath mafic and ultramafic rocks[34] during rifting. Mineral assemblages preserved in the gneisses of the lower plates record stages of partial re-equilibration on ascent towards the surface[13]. *P–T* paths suggest nearly adiabatic decompression at high temperatures, so residence time outside the eclogite stability field must have been short in order to escape total obliteration of high-pressure minerals. Encapsulation of high-pressure minerals and zircon inclusions in strong, fluid impermeable garnet hosts aided in their preservation[35]. In eastern PNG, preservation of relics of high-pressure mineral assemblages in retrogressed blueschists in the Dayman dome[20] and Normanby Island[36] also requires rapid exhumation at plate tectonic rates, especially since the present-day Mohorovičić discontinuity (Moho) is elevated relative to crust north and south of the core complexes[37]. Some of the deeply subducted material may have retraced its path by moving rapidly back up the subduction channel[4,35] at the same time that the spreading tip was propagating westwards. We infer that rifting reactivated structures within a former plate boundary that previously separated sediments and basalts of largely Australian affinity from overthrust ophiolitic rocks of the Papuan ultramafic belt.

Implications for eclogite exhumation

The D'Entrecasteaux high-pressure rocks are transient crustal features presently exposed at the Earth's surface whose *P–T–t–D* histories reveal insights into the four-dimensional plate boundary evolution during the transition from subduction to rifting in eastern PNG. This transition was accompanied by an increase in the geotherm (that is, non-steady-state geothermal gradients; Fig. 2), as the plate boundary was reorganized during westward propagation of the Woodlark spreading centre into eastern PNG. As the spreading centre continues to propagate westwards, and crust continues to be thinned, the D'Entrecasteaux Islands would be expected to eventually subside and be thermally overprinted at low pressures owing to impingement of upwelling mantle asthenosphere. This geologic transience may in part explain why similar metamorphic core complexes are difficult to recognize in the geologic record of plate boundary zones.

In the obliquely convergent AUS–PAC plate boundary zone, the possible role of microplate rotation in eclogite exhumation at plate tectonic rates has important implications for models of exhumation of high-pressure and UHP rocks in other regions. In most high-pressure and UHP terranes geologists are left to infer what structural, petrologic, and thermochronologic data represent in terms of exhumation mechanisms and large-scale plate interactions. Models for the exhumation of UHP rocks generally call on the buoyancy of continental crust subducted to mantle depths as the main driving force for exhumation[38], which ultimately manifests itself as regurgitated buoyant crustal slices bound above and below by normal and reverse faults, respectively[35]. Although satisfactory when considered in a two-dimensional cross-sectional view, these models are difficult to reconcile in three dimensions without the presence of major transfer faults or invoking some element of rotation. An artefact of the buoyancy model is that the rocks become neutrally buoyant in the middle crust, thus requiring an additional mechanism to facilitate exhumation to the surface. In the case of the eastern PNG high-pressure rocks, a complex interaction of microplates within the larger AUS–PAC plate boundary zone plays an important role in their exhumation. Extension in the D'Entrecasteaux Islands may be kinematically linked to microplate rotation and the westward propagation of an oceanic spreading centre into previously subducted crust. For Paleozoic or older high-pressure rocks[39], *P–T–t–D* evidence for the plate boundary zone evolution may have long been obliterated and the transition between subduction and rifting may occur so rapidly that evidence for the timing of these events would potentially be obscured by analytical errors associated with isotopic ages. We note, however, that the average exhumation rate for this eclogite from Fergusson Island is comparable to those obtained from exhumed high-pressure and UHP rocks from other localities (such as Dora Maira and Kokchetav)[40,41]. Furthermore, it is comparable to exhumation rates of mid-crustal rocks from other portions of the obliquely convergent AUS–PAC plate boundary (for example, the Southern Alps of New Zealand)[42].

The $^{238}U/^{206}Pb$ zircon age of 4.33 $\pm$ 0.36 Myr indicates that the exhumed lower plate of the D'Entrecasteaux metamorphic core complexes contains the youngest eclogite known on Earth. It formed and was exhumed during the complex reorganization of the Australian–South Bismark–Solomon–Woodlark plate boundary zone of eastern PNG. Results indicate that eclogites can be exhumed at rates that are similar to those at which oceanic crust is created and/or consumed at plate boundaries ($>$1 cm yr^{-1}). □

Methods

Electron probe analysis

Mineral compositions used for thermobarometry were obtained on a $\sim$2-mm diameter garnet porphyroblast and its inclusions by wavelength-dispersive X-ray analysis using a fully automated JEOL 733 electron microprobe at the Rensselaer Polytechnic Institute operating at 15 kV and 21.0 nA. Mineral compositions are given in the Supplementary Information.

U–Th–Pb analysis

For U/Pb ion probe analyses polished thin sections were mounted in epoxy along with zircon standard AS-3, ultrasonically cleaned in 1 N HCl, and Au coated. U–Th–Pb isotopes were measured using the University of California Los Angeles Cameca IMS 1270 ion microprobe. The mass resolution (5,000) was sufficient to resolve important molecular interferences in the mass range analysed. During analysis, a 12.5-kV primary O^- beam was focused on a $\sim 10 \times 15$ μm area of sectioned zircon from which sputtered positive secondary ions were extracted. The sample surface was flooded with 3×10^{-5} torr O_2 pressure to enhance Pb yields and an aperture was used to block ions derived from the periphery of the ion pit. Analyses consisted of 20 cycles with count times ranging from 1 to 15 s depending on peak intensity for each element.

Trace and REE analysis

Trace and REE data were obtained using the University of California Los Angeles Cameca IMS 1270 ion microprobe. An O^- primary beam with a current of 10–11 nA and an accelerating voltage of 12–13 kV was used during analysis. Element to element oxide ratios were determined on doped standard glasses for La, Ce, Nd, Sm, Eu and Gd to correct for isobaric interference on heavier REE isotopes. Zircon and garnet concentrations were derived relative to NIST 610 standard glass concentration, using intensities normalized to ^{30}Si for both zircon and garnet. Beam diameter was focused to 30 μm on both grains and

standard glass. Analyses consisted of ten cycles with count times ranging from 0.5 to 10 s depending on peak intensity for each element. Individual concentration values and the standard deviation of the eight analyses for each element are given in the Supplementary Information.

Received 29 March; accepted 12 July 2004; doi:10.1038/nature02846.

1. Stein, S. & Sella, G. F. in *Plate Boundary Zones* (eds Stein, S. & Freymuller, J. T.) 1–26 (American Geophysical Union, Washington DC, 2002).
2. Benes, V., Scott, S. D. & Binns, R. A. Tectonics of rift propagation into a continental margin: Western Woodlark Basin, Papua New Guinea. *J. Geophys. Res.* **99,** 4439–4455 (1994).
3. Hill, K. C. & Hall, R. in *Mesozoic-Cenozoic Evolution of Australia's New Guinea Margin in a West Pacific Context* (eds Hillis, R. R. & Muller, R. D.) (The Geological Society of America, Boulder, CO, 2003).
4. Davies, H. L. Crustal structure and emplacement of ophiolite in southeastern Papua New Guinea. *Coll. Int. CNRS* **272,** 17–33 (1980).
5. Taylor, B., Goodliffe, A. M. & Martinez, F. How continents break up: Insights from Papua New Guinea. *J. Geophys. Res.* **104,** 7497–7512 (1999).
6. Taylor, B., Goodliffe, A. M., Martinez, F. & Hey, R. Continental rifting and initial sea-floor spreading in the Woodlark Basin. *Nature* **374,** 534–537 (1995).
7. Abers, G. A. in *Non-Volcanic Rifting of Volcanic Margins: A Comparison of Evidence from Land and Sea* (eds Wilson, R. C. L., Whitmarsh, R. B., Taylor, B. & Froitzheim, N.) 305–318 (The Geological Society of London, London, 2001).
8. Hill, E. J. Geometry and kinematics of shear zones formed during continental extension in eastern Papua New Guinea. *J. Struct. Geol.* **16,** 1093–1105 (1994).
9. Davies, H. L. & Warren, R. G. Origin of eclogite-bearing, domed, layered metamorphic complexes ("core complexes") in the D'Entrecasteaux Islands, Papua New Guinea. *Tectonics* **7,** 1–21 (1988).
10. Hill, E. J., Baldwin, S. L. & Lister, G. S. Unroofing of active metamorphic core complexes in the D'Entrecasteaux Islands, Papua New Guinea. *Geology* **20,** 907–910 (1992).
11. Baldwin, S. L., Lister, G. S., Hill, E. J., Foster, D. A. & McDougall, I. Thermochronologic constraints on the tectonic evolution of active metamorphic core complexes, D'Entrecasteaux Islands, Papua New Guinea. *Tectonics* **12,** 611–628 (1993).
12. Davies, H. L. & Warren, R. G. Eclogites of the D'Entrecasteaux Islands. *Contrib. Mineral. Petrol.* **112,** 463–474 (1992).
13. Hill, E. J. & Baldwin, S. L. Exhumation of high-pressure metamorphic rocks during crustal extension in the D'Entrecasteaux region, Papua New Guinea. *J. Metamorph. Geol.* **11,** 261–277 (1993).
14. Pegler, G., Das, S. & Woodhouse, J. H. A seismological study of the eastern New Guinea and western Solomon Sea regions and its tectonic implications. *Geophys. J. Int.* **122,** 961–981 (1995).
15. Tregoning, P. *et al.* Estimation of current plate motions in Papua New Guinea from Global Positioning System observations. *J. Geophys. Res.* **103,** 12181–12203 (1998).
16. Weiler, P. D. & Coe, R. S. Rotations in the actively colliding Finisterre Arc Terrane: paleomagnetic constraints on Plio-Pleistocene evolution of the South Bismark microplate, northeastern Papua New Guinea. *Tectonophysics* **316,** 297–3251 (2000).
17. Hall, R. & Spakman, W. in *Mantle Structure and Tectonic Evolution of the Region North and East of Australia* (eds Hillis, R. R. & Muller, R. D.) 361–381 (The Geological Society of America, Boulder, Colorado, 2003).
18. Cooper, P. & Taylor, B. Seismotectonics of New Guinea: a model for arc reversal following arc-continent collision. *Tectonics* **6,** 53–67 (1987).
19. Abers, G. A. & Roecker, S. W. Deep structure of an arc-continent collision: earthquake relocation and inversion for upper mantle P and S wave velocities beneath Papua New Guinea. *J. Geophys. Res.* **96,** 6379–6401 (1991).
20. Worthing, M. A. Petrology and tectonic setting of blueschist facies metabasites from the Emo metamorphics of Papua New Guinea. *Aust. J. Earth Sci.* **35,** 159–168 (1988).
21. Davies, H. L. & Smith, I. E. Geology of eastern Papua. *Bull. Geol. Soc. Am.* **82,** 8299–8312 (1971).
22. Davies, H. L. & Ives, D. J. The geology of Fergusson and Goodenough Islands, Papua New Guinea. *Aust. Bur. Miner. Resour. Rep.* **82,** 1–83 (1965).
23. Zhang, R. Y. & Liou, J. G. in *Ultra-High Pressure Metamorphism and Geodynamics in Collision-Type Orogenic Belts; Final Report of the Task Group III-6 of the International Lithosphere Project* (eds Ernst, W. G. & Liou, J. G.) 216–228 (International Book Series 4, Bellwether Publishing for the Geological Society of America, Columbia, Maryland, 2000).
24. Ellis, D. J. & Green, D. H. An experimental study of the effect of Ca upon the garnet-clinopyroxene Fe-Mg exchange equilibria. *Contrib. Mineral. Petrol.* **71,** 13–22 (1979).
25. Powell, R. Regression diagnostics and robust regression in geothermometer/geobarometer calibration: the garnet-clinopyroxene geothermometer revisited. *J. Metamorph. Geol.* **3,** 231–243 (1985).
26. Holland, T. J. B. The reaction albite = jadeite + quartz determined experimentally in the range 600–1200°C. *Am. Mineral.* **65,** 129–134 (1980).
27. Gasparik, T. & Lindsley, D. L. in *Pyroxenes: Reviews in Mineralogy* (ed. Prewitt, C. T.) 309–340 (Mineralogical Society of America, Washington DC, 1980).
28. Schmitt, A. K. *et al.* The Geysers-Cobb Mountain-Magma System, California (Part 1): U-Pb zircon ages of volcanic rocks, conditions of zircon crystallization and magma residence times. *Geochim. Cosmochim. Acta* **67,** 3423–3442 (2003).
29. Cherniak, D. J. & Watson, E. B. Pb diffusion in zircon. *Contrib. Mineral. Petrol.* **172,** 198–207 (2000).
30. Hoskin, P. W. O. & Schaltegger, U. in *Zircon* (eds Hanchar, J. M. & Hoskin, P. W. O.) 27–62 (Mineralogical Society of America, Washington DC, 2003).
31. McDonough, W. F. & Sun, S.-S. The composition of the Earth. *Chem. Geol.* **120,** 223–253 (1995).
32. Rubatto, D. Zircon trace element geochemistry: partitioning with garnet and the link between U-Pb ages and metamorphism. *Chem. Geol.* **184,** 123–138 (2002).
33. Rubatto, D. & Hermann, J. Zircon formation during fluid circulation in eclogites (Monviso, Western Alps): implications for Zr and Hf budget in subduction zones. *Geochim. Cosmochim. Acta* **67,** 2173–2187 (2003).
34. Martinez, F., Goodliffe, A. M. & Taylor, B. Metamorphic core complex formation by density inversion and lower-crust extrusion. *Nature* **411,** 930–934 (2001).
35. Ernst, W. G. in *Physics of the Earth and Planetary Interiors: Processes and Consequences of Deep Subduction* (eds Rubie, D. C. & van der Hilst, R. D.) 253–276 (Elsevier, Amsterdam, 2001).
36. Baldwin, S. L., Fitzgerald, P. G., Little, T. A., Webb, L. E. & Monteleone, B. D. Exhumation of the youngest high-pressure rocks, at plate tectonic rates, during Plio-Pleistocene continental extension in SE Papua New Guinea. *Geol. Soc. Am. Abstr. Programs* **35,** 556 (2003).
37. Abers, G. A. *et al.* Mantle compensation of active metamorphic core complexes at Woodlark rift in Papua New Guinea. *Nature* **418,** 862–865 (2002).
38. Platt, J. P. Exhumation of high-pressure rocks:a review of concepts and processes. *Terra Nova* **5,** 119–133 (1993).
39. Maruyama, S., Liou, J. G. & Terabayashi, M. Blueschists and eclogites of the world and their exhumation. *Int. Geol. Rev.* **38,** 485–594 (1996).
40. Rubatto, D. & Hermann, J. Exhumation as fast as subduction? *Geology* **29,** 3–6 (2001).
41. Hacker, B. R., Calvert, A. J., Zhang, R. Y., Ernst, W. G. & Liou, J. G. Ultrarapid exhumation of ultrahigh-pressure diamond-bearing metasedimentary rocks of the Kokchetav Massif, Kazakhstan. *Lithos* **70,** 61–75 (2003).
42. Little, T. A., Cox, S., Vry, J. K. & Batt, G. Variations in exhumation level and uplift-rate along the oblique-slip Alpine fault, central Southern Alps, New Zealand. *Geol. Soc. Am. Bull.*(in the press).
43. Shipboard Scientific Party, in *Proc. ODP. Init. Rep. 180* (eds Taylor, B., Huchon, P. & Klaus, A.) 1–77 (Ocean Drilling Program, College Station, Texas, 1999).

Supplementary Information accompanies the paper on **www.nature.com/nature**.

Acknowledgements S.L.B. and P.G.F. gratefully acknowledge support from the US National Science Foundation's Geoscience Directorate, Division of Earth Sciences, Tectonics and Instrumentation and Facilities Programs. M.G. acknowledges support from the Department of Energy. Fieldwork would not have been successful without the efforts of D. Pinasi, and the support from City Resources. A. Schmitt contributed significantly in helping us to obtain ion microprobe REE analyses from zircon and garnet. The ion microprobe facility at UCLA is partly supported by a grant from the Instrumentation and Facilities Program, Division of Earth Sciences, US National Science Foundation.

Competing interests statement The authors declare that they have no competing financial interests.

Correspondence and requests for materials should be addressed to S.L.B. (sbaldwin@syr.edu).